THE JOURNAL OF BIOLOGICAL CHEMISTRY VOL. 289, NO. 19, pp. 13519–13530, May 9, 2014

High Glucose-induced *O*-GlcNAcylated Carbohydrate Response Element-binding Protein (ChREBP) Mediates Mesangial Cell Lipogenesis and Fibrosis

*THE POSSIBLE ROLE IN THE DEVELOPMENT OF DIABETIC NEPHROPATHY**

Received for publication, October 25, 2013, and in revised form, March 7, 2014 Published, JBC Papers in Press, March 10, 2014, DOI 10.1074/jbc.M113.530139

Min-Jung Park[‡], Dong-Il Kim[‡], Seul-Ki Lim[‡], Joo-Hee Choi[‡], Ho-Jae Han[§], Kyung-Chul Yoon[¶], and Soo-Hyun Park[‡1]

From the [‡]Department of Veterinary Physiology, College of Veterinary Medicine, Chonnam National University, Gwangju 500-757, Korea, the [§]Department of Veterinary Physiology, College of Veterinary Medicine, Seoul National University, Seoul 151-741, Korea, and the [¶]Department of Ophthalmology, Chonnam National University Medical School and Hospital, Gwangju 501-757, Korea

Background: Abnormal lipid synthesis and fibrosis can lead to diabetic nephropathy.
Results: High glucose-induced *O*-GlcNAcylated ChREBP increases the expression of lipogenic and fibrotic proteins and induces lipid accumulation and fibrosis.
Conclusion: *O*-GlcNAcylated ChREBP mediates lipogenesis and fibrosis in mesangial cells.
Significance: This is the first report that *O*-glycosylated ChREBP plays a pathophysiological role in lipogenesis and fibrosis in mesangial cells.

Carbohydrate response element-binding protein (ChREBP) is a transcription factor responsible for carbohydrate metabolism in the liver. However, the role of ChREBP in diabetic nephropathy has not been elucidated. Thus, we investigated the role of ChREBP in mesangial cells in diabetic nephropathy. Treatment with 25 mM glucose (high glucose; HG) increased cellular *O*-GlcNAc and *O*-GlcNAcylated ChREBP in mesangial cells compared with normal 5.5 mM glucose. *O*-(2-acetamido-2-deoxy-D-glucopyranosylidene) amino *N*-phenylcarbamate (PUGNAc), a drug that increases *O*-GlcNAc, augmented the expression of ChREBP targets, whereas DON, a drug that decreases *O*-GlcNAc and *O*-GlcNAcase overexpression, mitigated the increase with HG. *O*-GlcNAc augmented the protein stability, transcriptional activity, and nuclear translocation of ChREBP. HG treatment also stimulated lipid accumulation and the contents of triglyceride and cholesterol in mesangial cells. In addition, HG triggered expression of hypoxia-inducible factor 1-α, vascular endothelial growth factor, and extracellular matrix components related to nephrosclerosis. The ChREBP mutant, W130A, did not exhibit HG-induced lipid accumulation and fibrotic proteins, suggesting that the Trp-130 residue in the MCR3 domain is important in the development of glomerulosclerosis. *O*-GlcNAcylated ChREBP was elevated in mesangium cells of streptozotocin-induced diabetic rats. In conclusion, HG increased the *O*-GlcNAcylated ChREBP level, which resulted in lipid accumulation and up-regulation of fibrotic proteins in mesangial cells. These effects may lead mesangial cells to an ultimately pathological state.

Diabetic nephropathy is a major complication of diabetes mellitus, resulting in high mortality. Hyperglycemia is a primary factor in the development of diabetic nephropathy (1). Abnormal lipid metabolism and renal accumulation of lipids have been proposed to affect the progression of diabetic nephropathy (2–5). Recently, Kiss *et al.* (6) reported that lipid droplet accumulation in glomeruli is associated with an increase in hyperglycemia-induced renal damage, suggesting a pathophysiological role for lipid accumulation in mesangial cells in diabetic nephropathy. Therefore, understanding lipid metabolism in mesangial cells under a high glucose condition is necessary to comprehend the progress of nephropathy.

Emerging data indicate that GlcNAcylation may play an important role in diabetes. The hexosamine biosynthetic pathway is a branch of the glucose metabolic pathway, consuming approximately 2–5% of total glucose. *O*-GlcNAc levels in key cellular proteins, including *O*-GlcNAc transferase (OGT),[2] can be modulated by altering the extracellular glucose levels (7–11); thus, *O*-GlcNAc is hypothesized to be a nutritional sensor in the liver (12). Many reports indicate that *O*-GlcNAcylation is altered in metabolic diseases, such as diabetes (10, 12–16). Among the proteins associated with glucose metabolism, nuclear receptor liver X receptor is *O*-GlcNAc-modified in response to glucose (11). In addition, *O*-GlcNAc modification is essential for the glucose response of carbohydrate response element-binding protein (ChREBP), which controls the expres-

* This work was supported by Korean Science and Engineering Foundation Grant 2011-0016649.
[1] To whom correspondence should be addressed: Dept. of Veterinary Physiology, College of Veterinary Medicine, Chonnam National University, Gwangju 500-757, Korea. Tel.: 82-62-530-2832; Fax: 82-62-530-2809; E-mail: parksh@chonnam.ac.kr.

[2] The abbreviations used are: OGT, *O*-GlcNAc transferase; ChREBP, carbohydrate response element-binding protein; ChoRE, carbohydrate response element; SREBP, sterol regulatory element-binding protein; Mlx, Max-like protein X; ACC, acetyl-CoA carboxylase; FAS, fatty acid synthase; OGA, *O*-GlcNAcase; L-PK, L-type puruvate kinase; PUGNAc, *O*-(2-acetamido-2-deoxy-D-glucopyranosylidene) amino *N*-phenylcarbamate; HIF, hypoxia-inducible factor; STZ, streptozotocin; LG, low glucose; HG, high glucose; CHX, cycloheximide; MCR, Mondo conserved region; HRE, hypoxia-responsive element; DON, 6-diazo-5-oxo-L-norleucine.

sion of carbohydrate response element (ChoRE)-containing genes (17).

ChREBP is a basic helix-loop-helix leucine zipper transcription factor, a major mediator of glucose action in the liver, and regulates glucose homeostasis in cells with sterol regulatory element-binding protein (SREBP), primarily in the liver (18, 19). As the glucose level rises, ChREBP translocates from the cytosol into the nucleus and forms a heterodimer with Max-like protein X (Mlx) (20) to bind to ChoRE for transcriptional regulation of its target genes, which are particularly associated with glycolysis (L-type puruvate kinase; L-PK (21); lipogenesis (acetyl-CoA carboxylase (ACC) and fatty acid synthase (FAS) (22)); and transport, development, and cell motility (23). As mentioned above, indirect evidence indicates that ChREBP is modified by OGT/*O*-GlcNAcase (OGA) or its inhibitor, DON/PUGNAc, and other studies reported this ChREBP modification affects its stability, transcriptional activity, glucose utilization, and lipid synthesis in the liver (17, 24, 25). Although studies of ChREBP function in the kidney are limited, the augmented expression of ChREBP in kidneys of rats with chronic renal failure has been reported (26). Isoe *et al.* (27) recently reported hypoxia-inducible factor 1-α (HIF-1α) regulation of ChREBP in glomerular mesangial cells. In cultured mesangial cells, high glucose enhances the expression of HIF-1α and its target genes involved in the development of diabetic glomerulopathy (27). Therefore, in this study, we examined the role of ChREBP in lipid accumulation and renal fibrosis in mesangial cells. Furthermore, we investigated the role of GlcNAcylation of ChREBP in the progression of diabetic nephropathy, especially in renal fibrosis.

EXPERIMENTAL PROCEDURES

Antibodies and Reagents—All chemicals were obtained from Sigma-Aldrich with the exception of the following: Dulbecco's modified Eagle's medium (with low glucose or no glucose) and fetal bovine serum (Invitrogen); PUGNAc (Toronto Research Chemicals, Ontario, Canada); HIF-1 inhibitor (Santa Cruz Biotechnology, Inc., catalogue no. sc-221724); and Protein A/G PLUS-agarose (Santa Cruz Biotechnology). Antibodies against β-actin, lamin B, *O*-GlcNAc (RL-2), 14-3-3, collagen IV, tubulin, ChREBP (for the proximity ligation assay), and goat IgG were purchased from Santa Cruz Biotechnology. Antibodies against OGT, FAS, VEGF, and HA were purchased from Abcam (Cambridge, MA). Antibodies against ACC, rabbit IgG, and mouse IgG were purchased from Cell Signaling Technology (Beverly, MA). Anti-ChREBP (from Novus Biologicals, except for the proximity ligation assay), anti-fibronectin (BD Biosciences), anti-HIF-1α (Thermo Scientific), and anti-FLAG M2 (Sigma) were obtained from the indicated sources.

Cell Lines and Cell Culture Conditions—Rat mesangial cells and HEK293 cells were purchased from ATCC (CRL-2573^{TM} and CRL-1573^{TM}, respectively). The culture medium for the cells was DMEM, 5.6 mmol/liter glucose, supplemented with 10% fetal bovine serum, streptomycin (100 μg/ml), and penicillin (100 units/ml) at 37 °C in 95% air, 5% CO_2. The media were changed every other day. Nearly confluent cells were incubated for 16 h in serum-free medium prior to treatment. Experimental medium was DMEM with low glucose (5.6 mmol/liter) with or without additional an 20 mmol/liter D-glucose or DMEM without glucose (Invitrogen, catalogue no. 11966-025) and lasted 24 h.

Construction of ChREBP Plasmids and Luciferase Assay—Each FLAG-tagged ChREBP wild type and W130A mutant in CMVS4 vector, HA-tagged Max-like protein X (Mlx) γ, and 2× ACC ChoRE/PK(−40) luciferase plasmid (28) were generously provided by Dr. Howard C. Towle (University of Minnesota, Minneapolis, MN) (20). The mesangial cells were transiently transfected with ChREBP wild type or W130A or empty vector plasmids in addition to Mlx, β-galactosidase, and luciferase plasmids. After 24 h, the culture medium was replaced with medium containing the indicated concentrations of glucose and incubated for an additional 24 h. β-Galactosidase plasmid was used as a control for the normalization of transfection efficiency.

Protein Extraction and Western Blotting—The cell pellet or kidney cortex was lysed in NE-PER nuclear and cytoplasmic extraction reagents (Thermo Scientific) or M-PER mammalian protein extraction reagent (Thermo Scientific) containing protease inhibitor mixture (Sigma) and phosphatase inhibitor mixture I + II (Sigma), and fractional protein was extracted according to the manufacturer's instructions. The protein level was quantified using the Bradford procedure. 30 μg of whole cell extracts, cytoplasmic extracts, or nuclear extracts were separated by SDS-PAGE and transferred to an enhanced nitrocellulose membrane. The blots were then washed with TBST (10 mM Tris-HCl, pH 7.6, 150 mM NaCl, 0.1% Tween 20), blocked with 5% skim milk for 1 h, and incubated overnight at 4 °C with the primary antibody at the dilutions recommended by the supplier. The membrane was then washed with TBST, and the secondary antibodies conjugated to horseradish peroxidase were incubated for 1 h at room temperature. The bands were visualized using EZ-Western Lumi Pico Western blotting detection reagents (Daeillab Service Co., Seoul, Korea) on x-ray film (Eastman Kodak Co. BioMax light film) or a luminescent image analyzer (ImageQuant LAS4000 mini, GE Healthcare).

RNA Preparation, RT-PCR, and Quantitative RT-PCR—Total RNA was extracted from the cells using TRIzol according to the manufacturer's instructions (Invitrogen). Reverse transcription was carried out with 1 μg of total RNA using an RT Premix reverse transcription system kit (AccuPower, Seoul, Korea) with oligo$(dT)_{18}$ primers. 2 μl of the RT products was amplified with a PCR Premix kit (AccuPower, Seoul, Korea). The PCR primer sequences are presented in Table 1. β-Actin was used as a control to confirm the quantity of the RNA. The RT-PCR products were separated and visualized on 1.2% agarose gels. 0.5 μl of the RT products was amplified with Power SYBR Green (Applied Biosystems, Warrington, UK). The primers used are indicated in Table 1. The quantitative RT-PCR products were analyzed using a StepOne^{TM} real-time PCR system (Applied Biosystems, Invitrogen). All samples were analyzed in triplicate and expressed as mean ± S.E.

Cloning and DNA Transfection—*Ogt* and *Oga* genes (National Institutes of Health mammalian gene collection) were obtained from Invitrogen. *Ogt* insert DNA was generated by PCR using primers 5′-aagtcgaccatggcgtcttccgtgggcaac-3′ and

TABLE 1
Primer sequences used in this study

Gene	Forward	Reverse
ChREBP	5′-AGACCCAAAGACCAAGATG-3′	5′-TTCTGACAACAAAGCAGGA-3′
Acc	5′-ACAGTGGAGCTAGAATTGGAC-3′	5′-ACTTCCCGACCAAGGACTTTG-3′
Fas	5′-CACATCAAGTGGGACCAC-3′	5′-ACTCACACCCACCCAGA-3′
L-PK	5′-AGTGACGTGTTAGCAGTCCG-3′	5′-CTGTGTGGCACAAACGACAG-3′
O-GlcNAcase (*MGEA5*)	5′-GCAGAAGGAGAGTCAAGCGA-3′	5′-TGCACCCAAACTGAGAAACC-3′
O-GlcNAc transferase	5′-TTTCAATGCACAAGGGGAAA-3′	5′-CAGAGAGTCTGCATGGGTGG-3′
Hif-1α	5′-GTAATGTTCCCCTCTTCTAATG-3′	5′-ACTCTGGGCTTGACTCTAACT-3′
Vegfα	5′-GTCCTGTGTGCCCCTAATGC-3′	5′-ATGTGCTGGCTTTGGTGAGG-3′
Fibronectin	5′-CGCGGTTTTGGTTCAGACTC-3′	5′-GGCATCGTAGTTCTGGGTGG-3′
Collagen 1A1	5′-GGCAAAGATGGACTCAACGG-3′	5′-GTCATAACCACCGCTGGGAG-3′
Collagen 3A1	5′-CACCTGGCAAAAACGGAGA-3′	5′-AGCGTCTCCCTTGTCACCAG-3′
Collagen 4A1	5′-AACGGCATTGTGGAGTGTCA-3′	5′-CTGTCCAACTTCGCCTGTCA-3′
β-Actin	5′-AGGCCCAGAGCAAGAGAG-3′	5′-TCAACATGATCTGGGTCATC-3′

5′-aagcggccgcttatgctgactcagtgacttc-3′ from pOTB7-hOGT as a template. *Ogt* insert DNA was generated by PCR using primers 5′-aagtcgaccatggtgcagaaggagagtca-3′ and 5′-aagcggccgctcacaggctccgaccaagta-3′ from pCMV-SPORT6-hOGA as a template. Each amplified fragment was digested with SalI and NotI and inserted into pCMV-HA, respectively. Mesangial cells were stabilized for 24 h before they were transfected with the DNAs. The culture medium was exchanged, and the constructs were transfected into the mesangial cells using GeneExpresso Max transfection reagent (Excellgen, Rockville, MD), as instructed by the manufacturers.

Immunoprecipitation—Cells were co-transfected with FLAG-tagged ChREBP and HA-tagged Mlx using GeneExpresso Max transfection reagent (Excellgen, Rockville, MD). After 24 h, cells were collected in 50 mM Tris-Cl (pH 7.5), 150 mM NaCl, 1 mM EDTA, 1% Nonidet P-40 with protease inhibitors and then lysed by vortexing. Equal amounts of lysate were incubated overnight with 2 μg of primary antibody rotating at 4 °C, followed by incubation with 30 μl of protein A/G PLUS-agarose (Santa Cruz Biotechnology) for 2 h at 4 °C. Immunoprecipitates were extensively washed, resuspended in 2× sample buffer, boiled for 5 min, and analyzed by immunoblotting. Nuclear extracts of kidney cortexes from streptozotocin-induced diabetic rats or normal rats were immunoprecipitated under the same protocol described above.

Immunofluorescence—Mesangial cells were fixed with 4% paraformaldehyde in phosphate-buffered saline (PBS), followed by permeabilization with 0.1% (v/v) Triton X-100, and washed three times for 10 min each with PBS. Cells were incubated for 1 h with 5% (v/v) BSA in PBS and incubated overnight with anti-ChREBP primary antibody (1:500) in a solution containing 5% (v/v) BSA in PBS and washed three times for 10 min each with PBS. Cells were incubated with a secondary FITC-conjugated anti-rabbit IgG antibody (Sigma-Aldrich) for an additional 1 h. Nuclei were stained with 4′,6-diamidino-2-phenylindole (DAPI) during the final incubation step. Cells were imaged using a microscope (Nicon Te-300, Nicon (Melville, NY)).

Oil Red O Staining—Cells were fixed in 4% paraformaldehyde in PBS for 10 min, washed with 60% isopropyl alcohol. Then the cells were stained for 10 min in 0.2% Oil Red O dissolved in 60% isopropyl alcohol and washed four times with distilled water, followed by additional hematoxylin staining for 30 s and washed four times with water. Cells were imaged using a microscope (Leica DM IRB, Leica Microsystems Inc. (Deerfield, IL)).

Picrosirius Red Staining—Cells cultured on coverglass with or without additional 30 mM glucose were fixed in 4% paraformaldehyde for 10 min and washed with distilled water. Staining was performed using the Picrosirius Red stain kit (Polysciences, Warrington, PA) according to the manufacturer's instructions. Stained cells were mounted and imaged using a microscope (Nicon Te-300, Nicon).

Proximity Ligation Assay—An *in situ* proximity ligation assay was performed in adult male Sprague-Dawley rats. Diabetes was induced by injection of streptozotocin (STZ; 35 mg/kg, intraperitoneally) dissolved in cold and fresh citrate buffer (0.1 M and pH 4.5). After 2 weeks, all rats were sacrificed, and kidney was extracted. Experiments were performed in accordance with National Institutes of Health animal research standards, and protocols were approved by the Chonnam National University Laboratory Animal Research Center. Fixed kidneys in 10% neutral buffered formalin were embedded in paraffin and cut at a 10-μm thickness. Paraffin sections were deparaffinized with Histochoice (Amresco) and rehydrated with serial diluted ethanol. Sections were steamed in sodium citrate buffer (10 mM sodium citrate, 0.05% Tween 20, pH 6.0) for antigen retrieval and washed with PBS. Then a proximity ligation assay was performed using Duolink (Olink Biosciences, Uppsala, Sweden) according to the manufacturer's instructions. Briefly, the sections were incubated with primary antibodies (anti-ChREBP and RL-2), diluted to 1:20 in antibody diluents supplied, overnight at 4 °C. The Duolink proximity ligation assay probes were incubated in a preheated humidity chamber for 1 h at 37 °C, and then, ligation and amplification were performed. To reduce tissue autofluorescence, sections were incubated with copper sulfate (5 mM $CuSO_4$ in 50 mM ammonium acetate buffer, pH 5.0) for 20 min (29), followed by mounting with ProLong® Gold antifade reagent with DAPI (Invitrogen). The stained sections were observed using a BX-40 apparatus (Olympus, Tokyo, Japan) with an eXcope X3 digital camera (DIXI Optics, Daejeon, South Korea).

Quantitation of Triglyceride and Cholesterol—The contents of triglyceride and cholesterol were determined using colorimetric kits (BioVision) according to the manufacturer's instructions. For triglyceride quantification, cells cultured on 10-cm dishes were homogenized in a 1-ml solution containing 5% Nonidet P-40 in water, heated to 100 °C in a water bath for 5

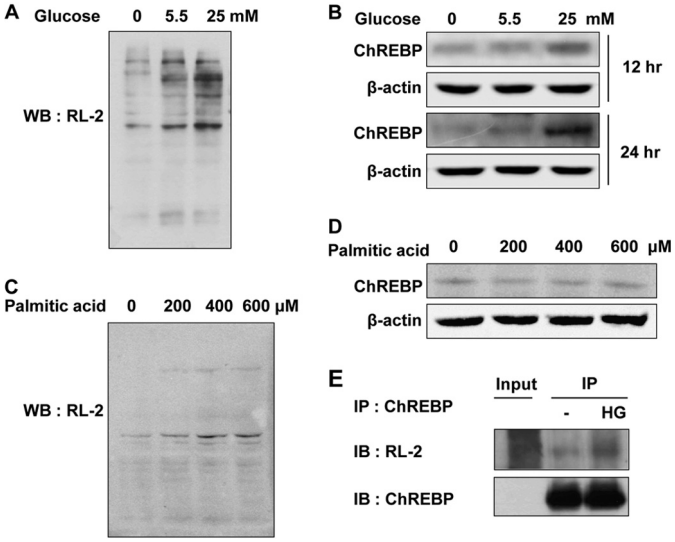

FIGURE 1. ***O*-GlcNAc modification of ChREBP in mesangial cells under high glucose.** *A*, mesangial cells were exposed to the 0, 5.5, or 25 mM glucose for 24 h, and the cells were assessed for the *O*-GlcNAc-modified protein pools by immunoblotting (*IB*) using RL-2 antibodies specific to *O*-GlcNAc. *B*, mesangial cell ChREBP levels, according to the glucose concentration levels, were determined by immunoblotting. *C* and *D*, the *O*-GlcNAc-modified protein pools and ChREBP levels under palmitic acid were determined. The data are normalized by the quantities of β-actin. *E*, HA-ChREBP-transfected mesangial cells were treated with or without 25 mM glucose (HG) for 24 h. Cell lysates were immunoprecipitated (*IP*) with ChREBP antibodies and probed with RL-2 antibodies.

min, and then cooled down to room temperature two times. Samples were centrifuged, and the supernatants were diluted 10-fold with water. For cholesterol quantification, cells were extracted with chloroform/isopropyl alcohol/Nonidet P-40 in a microhomogenizer. Samples were centrifuged at 15,000 × *g* for 10 min, and supernatants were dried under vacuum for 30 min to remove organic solvent. Dried lipids were dissolved with cholesterol assay buffer. Absorbance was measured at 570 nm.

Statistical Analysis—The results were expressed as the mean ± S.E. Values are the mean ± S.E. of three or four independent experiments. All of the experiments were analyzed by analysis of variance. In some experiments, such as RT-PCR and Western immunoblotting using inhibitors, a comparison of the treatment means was made with the control using the Bonferroni-Dunn test. A p value of <0.05 was considered significant.

RESULTS

O-GlcNAc Modification of ChREBP in Mesangial Cells under the High Glucose Condition—We first examined whether *O*-GlcNAc in mesangial cells was altered in diabetes. We treated mesangial cells with 0, 5.5 (low glucose; LG), or 25 mM glucose (high glucose; HG) for 24 h and monitored the increase of *O*-GlcNAc modification under the HG condition, which mimics a diabetic glucose concentration (Fig. 1*A*). Among proteins related to glucose metabolism, ChREBP, which acts as a glucose sensor, is regulated by *O*-linked GlcNAc modification (17). To determine whether ChREBP is regulated in mesangial cells under the HG condition, we evaluated ChREBP levels. The ChREBP level was increased under the HG condition (Fig. 1*B*), whereas palmitic acid did not increase the protein level, although palmitic acid moderately increased the *O*-GlcNAc pool in a concentration-dependent manner in mesangial cells (Fig. 1, *C* and *D*). Furthermore, ChREBP *O*-GlcNAcylation was increased under the HG condition compared with the LG condition based on immunoprecipitation with an anti-ChREBP antibody followed by immunoblotting with an anti-RL-2 antibody (Fig. 1*E*). This relationship between ChREBP and the HG condition in mesangial cells warranted further investigation as to whether ChREBP is regulated and plays a role in mesangial cells exposed to HG.

Effects of OGT and OGA Overexpression under the High Glucose Condition—To assess the effect of ChREBP *O*-GlcNAcylation under the HG condition in mesangial cells, the *OGT* or *Mgea5* (which codes for OGA) gene was transfected into mesangial cells. The HG-induced increase in the ChREBP mRNA level was unaffected by overexpression of either OGA or OGT, whereas HG induction of mRNAs of ChREBP target genes (*Acc*, *Fas*, and *L-pk*) was abolished by overexpression of OGA but not OGT (Fig. 2*A*). Instead, the HG-induced increase in the ChREBP level was affected by OGA (Fig. 2*B*). When cells were transfected with OGA or OGT, the expression of the other countergene was also increased modestly, possibly because alterations in OGT or OGA protein levels cause a reciprocal change in the expression of the other (30), which might partially explain this discrepancy. Then, when we examined ChREBP transcription using 2× ACC ChoRE/PK(−40) luciferase plasmid, which harbors the pyruvate kinase basal promoter (−40 to +12) driving luciferase expression (28), luciferase activity was increased under HG under both endogenous and exogenous conditions in a manner dependent on Mlx, the functional heteromeric partner of ChREBP (Fig. 2*C*). The increased activity under HG was abolished by ectopic expression of *OGA* and augmented synergistically by *OGT* overexpression, whereas the promoter activities were completely abolished by dominant negative ChREBP W130A, which is mutated in the Trp-130 residue of the MCR3 domain (31) (Fig. 2*D*). These results suggest that *O*-GlcNAcylation of ChREBP in response to HG plays a role in its activity in mesangial cells and that the Trp-130 residue in the MCR3 domain is important for this function, although the Trp-130 residue is an undefined site for direct *O*-GlcNAcylation.

O-GlcNAcylation of ChREBP Increases Expression of Its Target Genes—We used an OGA inhibitor, PUGNAc, and a GFAT inhibitor, DON, to elucidate the effect of ChREBP *O*-GlcNAcylation on gene expression. The ChREBP mRNA level was increased only upon HG treatment, independently of PUGNAc or DON, according to RT-PCR (Fig. 3*A*), and additional quantitative real-time PCR experiments confirmed HG-dependent and *O*-GlcNAc-independent ChREBP transcription. However, transcription of ChREBP target genes, such as *Acc*, *Fas*, and *Hif-1α*, were increased by PUGNAc and/or HG; this effect was prevented by pretreatment with DON (Fig. 3*B*), similar to previous transfection results (Fig. 2*B*). The transcription levels of these genes were significantly increased under the HG condition and to a greater extent compared with treatment with PUGNAc only. The responses to PUGNAc under the HG condition differed among the target genes; the *Fas* mRNA level

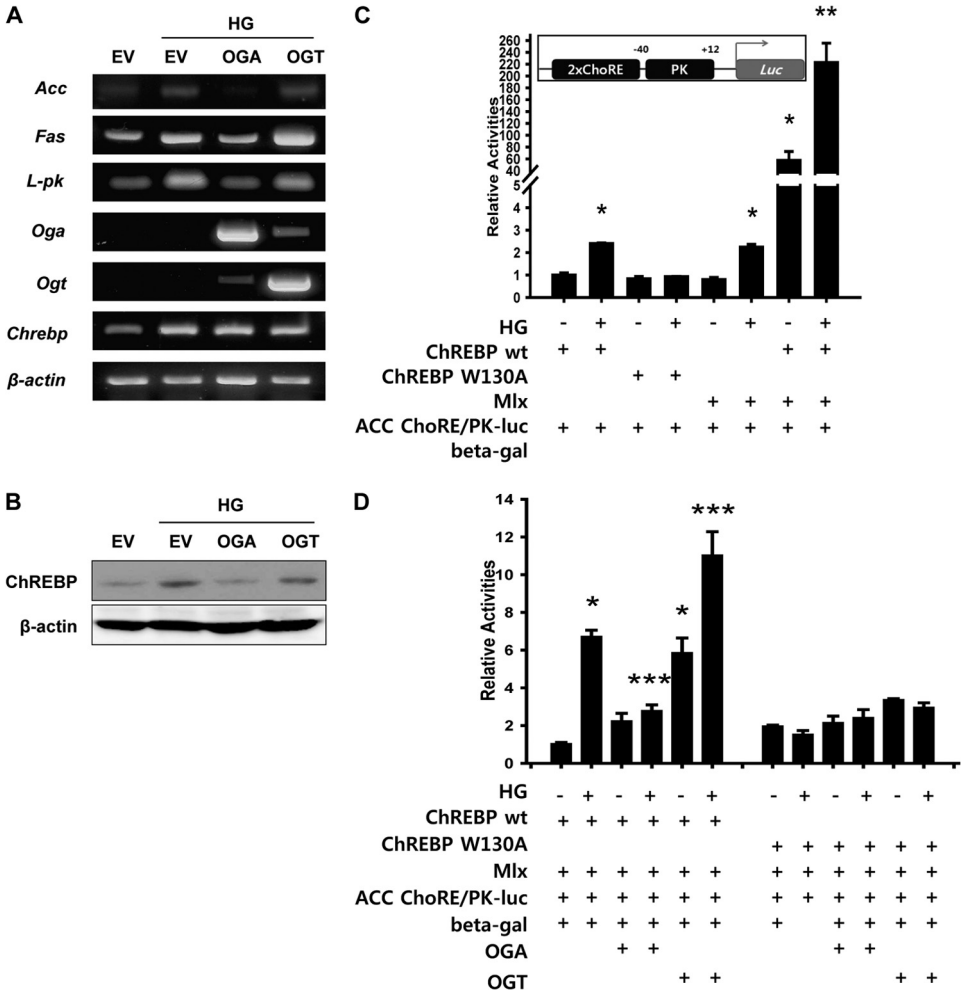

FIGURE 2. **Ectopic expression effects of OGT and OGA under the high glucose condition.** OGT- or OGA-transfected mesangial cells were treated with or without HG for 16 h. The mRNA (*A*) and protein (*B*) levels were determined by reverse transcription-PCR and immunoblotting. *C* and *D*, mesangial cells were co-transfected with ChREBP, Mlx, β-galactosidase expression vector, and luciferase reporter plasmid containing two copies of the ACC ChoRE. After 24 h, cells were treated with or without HG for 16 h. β-Galactosidase were used to normalize the transfection efficiency. Data are the mean ± S.E. (*error bars*) values of the activities of luciferase from three individual experiments. *, $p < 0.05$ *versus* control. **, $p < 0.05$ *versus* normal glucose control. ***, $p < 0.05$ *versus* no OGA- or OGT-transfected control.

was increased, whereas those of the other mRNAs were decreased modestly compared with under the HG condition only, suggesting another regulatory mechanism in addition to *O*-GlcNAc in mesangial cells under the HG condition. Additionally, the levels of ChREBP and its target proteins, ACC, FAS, and HIF-1α, were increased by PUGNAc and/or HG. Moreover, vascular endothelial growth factor-α (VEGFα), a target of HIF-1α, was induced in a pattern similar to ChREBP (Fig. 3*C*). However, levels of LXRα and SREBP-1c, regulators of both glucose and lipid metabolism mainly in the liver, were not altered significantly either by HG or inhibitors, and moreover, TXNIP, a target protein containing the ChoRE domain within its promoter region, was up-regulated under the HG condition but independently of use of the inhibitors. Additionally, we treated cells with HG with or without DON pretreatment after transfection of FLAG-wild type ChREBP, the FLAG-CREBP W130A mutant, or an empty vector with HA-Mlx in human embryonic kidney 293 (HEK293) cells to confirm the relevance of ChREBP and *O*-GlcNAc. As shown in Fig. 3*D*, ectopic expression of ChREBP increased ACC, FAS, HIF-1α, and VEGF levels; indeed, further synergistic increases were noted under the HG condition; these were blocked by pretreatment with DON. Furthermore, ectopic expression of ChREBP W130A mutant prevented the above described effects. These results indicate that both the level of the ChREBP protein and the transcription of the encoding gene are enhanced by HG and/or the HG-induced increase in *O*-GlcNAc in mesangial cells.

O-GlcNAcylation of ChREBP Increased Its Stability and Nuclear Localization—To further investigate the roles of *O*-GlcNAcylation in ChREBP stability in mesangial cells under the HG condition, we treated cells with cycloheximide (CHX), a translation inhibitor, which suppresses *de novo* protein synthesis. As shown in Fig. 4*A*, CHX treatment induced the degradation of ChREBP, and PUGNAc pretreatment dramatically increased CHX-induced stability of ChREBP under the LG condition, implying that *O*-GlcNAcylation prevents ChREBP degradation. Moreover, the ChREBP protein level was decreased slightly by CHX treatment under the HG condition, whereas DON treatment significantly abolished the increased protein level (*lane 2 versus lanes 6–8*). These results suggest that

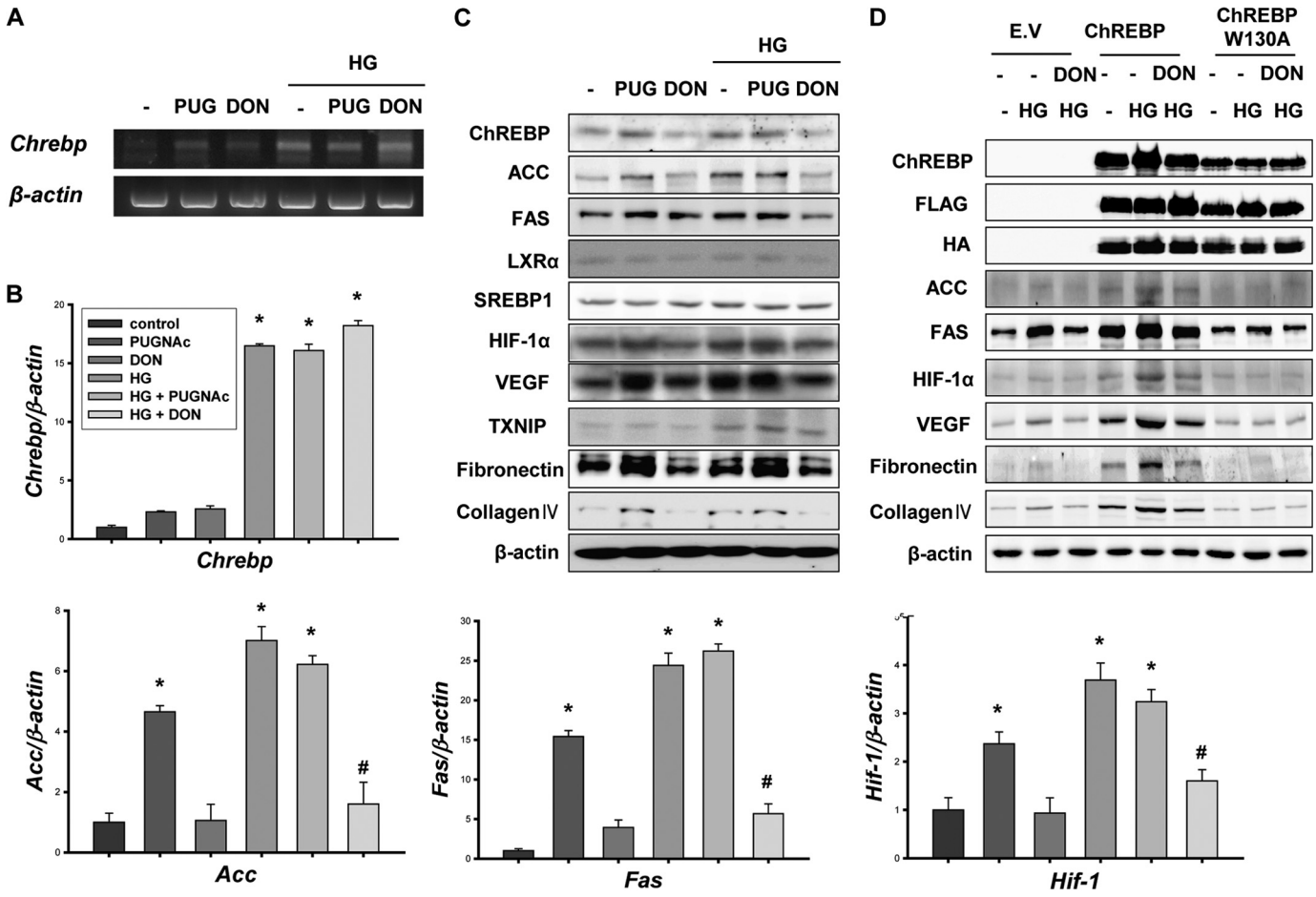

FIGURE 3. **O-GlcNAcylation of ChREBP increases expression of its target genes.** Mesangial cells were pretreated with or without 100 μM PUGNAc or 40 μM DON. After 15 min, cells were treated with HG for 16 h. The mRNA levels were determined by RT-PCR (*A*) and by real-time PCR (*B*). *C*, mesangial cells treated with PUGNAc or DON with or without HG for 24 h were determined by immunoblotting. *D*, empty vector (*E.V.*), wild type ChREBP, or mutant ChREBP W130A was transfected into HEK293 cells. After 24 h, cells were treated with PUGNAc or DON with or without HG for an additional 24 h. *Error bars*, S.E.

ChREBP stability is enhanced under the HG condition and that *O*-GlcNAcylation is important for maintenance of ChREBP stability.

Next, we examined ChREBP localization in mesangial cells following HG treatment. Even under the normal condition, ChREBP is scattered and shuttled between the cytosol and nucleus. Therefore, we investigated whether intracellular ChREBP localization in mesangial cells is altered due to *O*-GlcNAc under the HG condition. When mesangial cells were treated with HG for various periods of time, the nuclear ChREBP content was increased dramatically, particularly at 24 h (Fig. 4*B*), and the nucleus/cytosol ChREBP ratio was relatively high in the presence of PUGNAc with or without HG and low in the presence of DON, independently of HG (Fig. 4*C*). Immunofluorescence analysis of endogenous ChREBP showed that the overall ChREBP protein content was increased, and the protein was more concentrated in the nucleus of mesangial cells treated with HG or PUGNAc (Fig. 4*D*). These results suggest that *O*-GlcNAcylation affects the function of ChREBP by enhancing its stability and facilitating its shuttling to the nucleus.

Relation between O-GlcNAc and ChREBP Partners—Additionally, we performed co-transfection with FLAG-ChREBP and HA-Mlx in HEK293 cells followed by immunoprecipitation with an anti-FLAG antibody to investigate whether the interaction between ChREBP and Mlx is altered. The interaction between ChREBP and Mlx was augmented by PUGNAc or HG treatment compared with the control and DON treatment (Fig. 5*A*). These results suggest that HG-induced *O*-GlcNAcylation of ChREBP increased its transcriptional activity by regulating the interaction with Mlx, possibly due to a conformational change in ChREBP.

The 14-3-3 protein is proposed to sequester ChREBP in the cytosol (32), but other researchers have suggested that the Mondo conserved region (MCR) domain of ChREBP plays an essential role in glucose activation independently of its interaction with 14-3-3 (31); thus, the role of 14-3-3 remains controversial. Therefore, we evaluated the 14-3-3 protein level in mesangial cells. The 14-3-3 protein level was not affected by HG treatment or *O*-GlcNAc state; moreover no change in ChREBP binding with 14-3-3 protein under the HG condition was observed (Fig. 5, *B* and *C*). These results suggest that 14-3-3 is not regulated by HG-induced *O*-GlcNAc modification.

O-GlcNAcylation of ChREBP Induces Lipid Accumulation in Mesangial Cells—A number of clinical studies have shown that increased lipid levels are associated with accelerated progres-

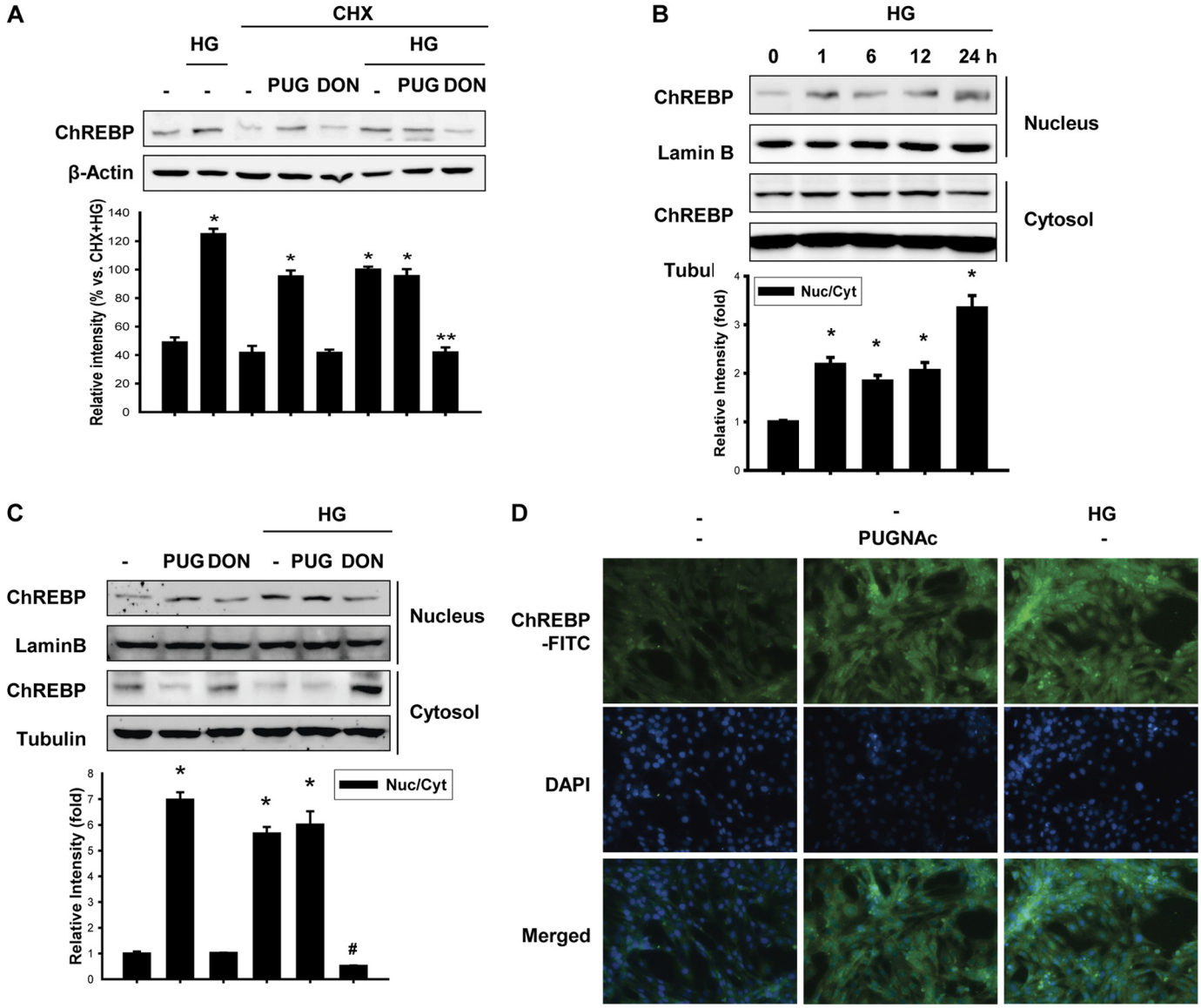

FIGURE 4. ***O*-GlcNAcylation of ChREBP increases its protein stability and nuclear localization.** *A*, mesangial cells were treated with drugs on the order of 10 μM CHX, 100 μM PUGNAc, or 40 μM DON and HG at intervals of 15 min as indicated. The protein levels of ChREBP were determined by immunoblotting. *B* and *C*, drug-treated mesangial cells, as indicated, were lysed and separated to cytosolic and nucleic proteins. Lamin B and tubulin were used to normalize the quantities of nucleic and cytosolic proteins, respectively. Each *lower panel* denotes the mean ± S.E. (*error bars*) of three experiments for each condition determined from densitometry relative to β-actin. *, $p < 0.05$, *versus* control. **, $p < 0.05$ *versus* HG with CHX. #, $p < 0.05$ *versus* HG alone. *D*, HG or PUGNAc-treated mesangial cells were labeled with anti-ChREBP and an FITC-conjugated secondary antibody. Nuclei were stained with DAPI and observed under a fluorescence microscope (magnification, ×200).

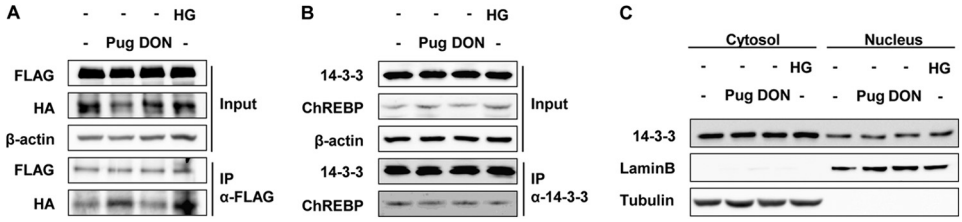

FIGURE 5. **Relation between *O*-GlcNAc and ChREBP partners.** ChREBP and Mlx co-transfected HEK293 cells (*A*) or non-transfected mesangial cells (*B*) were treated with HG, PUGNAc, or DON for 24 h. *A*, cell lysates were immunoprecipitated (*IP*) with FLAG antibodies and immunoblotted with FLAG or HA antibodies. *B*, cell lysate were immunoprecipitated with 14-3-3 antibodies and immunoblotted with 14-3-3 or ChREBP antibodies. *C*, fractionated mesangial cell proteins were determined by immunoblotting. Lamin B and tubulin were used to normalize the quantities of nucleic and cytosolic proteins, respectively.

sion of renal disease (4, 5, 33). Because the levels of ChREBP and its lipogenic target genes were augmented by PUGNAc and/or HG, we assayed lipid accumulation using Oil Red O staining to elucidate the pathophysiological function of ChREBP in mesangial cells. As shown in Fig. 6*A*, both PUGNAc and HG induced lipid accumulation compared with control or the HG condition

with DON pretreatment, similar to that facilitated by the saturated fatty acid, palmitic acid, which was used as the positive control. Moreover, lipid accumulation in ChREBP wild type-transfected HEK293 cells under the HG condition was prevented by pretreatment with DON; no such effects were observed in cells transfected with the ChREBP W130A mutant (Fig. 6*B*). To examine the type of lipids accumulated in mesangial cells, triglyceride and cholesterol quantification assays were performed. By PUGNAc or HG, triglyceride and cholesterol concentrations were about 60 and 100% increased, respectively, whereas they were decreased by HG with DON (Fig. 6, *C* and *D*), suggesting that increased ChREBP level and stability lead to accumulation of neutral lipid. Together, these results indicate that HG-induced *O*-GlcNAc could cause lipid accumulation through ChREBP modification, leading to further renal disease.

Hif-1α Induced by ChREBP Regulates Fibrosis-related Gene Expression in Mesangial Cells under High Glucose—The *Vegf* gene contains a hypoxia-responsive element (HRE) in the promoter region, suggesting that HIF-1α regulates VEGF transcription, and excess VEGF is considered relevant to the pathogenesis of diabetic nephropathy (34) and focal glomerular sclerosis (35). Recently, VEGF-induced fibronectin up-regulation was reported in mesangial cells (36). Therefore, we assayed the *Vegf* and fibronectin mRNA levels in the same context by real-time PCR. The *Vegf* and fibronectin transcription levels were increased by PUGNAc with or without HG (Fig. 7*A*), similar to *Hif-1α* (Fig. 3*B*). Furthermore, the expression level of non-fibrillary type-IV collagen, fibrillary type-I and -III collagens, and a myofibroblast marker, α-smooth muscle actin, also were increased by both PUGNAc and HG (Fig. 7*A*). A HIF-1α inhibitor, a cell-permeable amidophenolic compound that inhibits HIF-1 transcription and exerts no apparent effect on the cellular *Hif-1α* mRNA or HIF-1 level, prevented the HG-induced increases in VEGF, fibronectin, and collagen IV protein levels without affecting the ChREBP, ACC, FAS, or HIF-1α protein level (Fig. 7*B*). These findings suggest a role for *O*-GlcNAcylated ChREBP in HIF-1α-mediated fibrosis in mesangial cells under the HG condition. Consistent with those findings, picrosirius red staining showed that the increased fibrosis of mesangial cells induced by both PUGNAc and HG and fibrosis was prevented by HIF-1α inhibition (Fig. 7*C*). Therefore, in mesangial cells treated with HG, *O*-GlcNAc-modified ChREBP mediates lipogenesis and fibrosis by regulating ACC and FAS and regulating HIF-1α, respectively.

Elevated O-GlcNAcylated ChREBP in Mesangium Cells of Streptozotocin-induced Diabetic Rats—To determine whether ChREBP is actually *O*-GlcNAcylated *in vivo*, we examined the *O*-GlcNAcylated ChREBP within the mesangium of STZ-induced diabetic rats exhibiting significant hyperglycemia using an *in situ* proximity ligation assay with anti-ChREBP and RL-2 antibodies, to make ChREBP exhibit fluorescence when it is *O*-GlcNAcylated. As shown in Fig. 8*A*, mesangial cells within the mesangium of STZ-induced diabetic mice showed much more fluorescence, compared with those of control mice. Additionally, *O*-GlcNAcylated ChREBP from nuclear extracts of kidney cortexes of STZ rats was considerably higher than that from normal rats, examined by immunoprecipitation

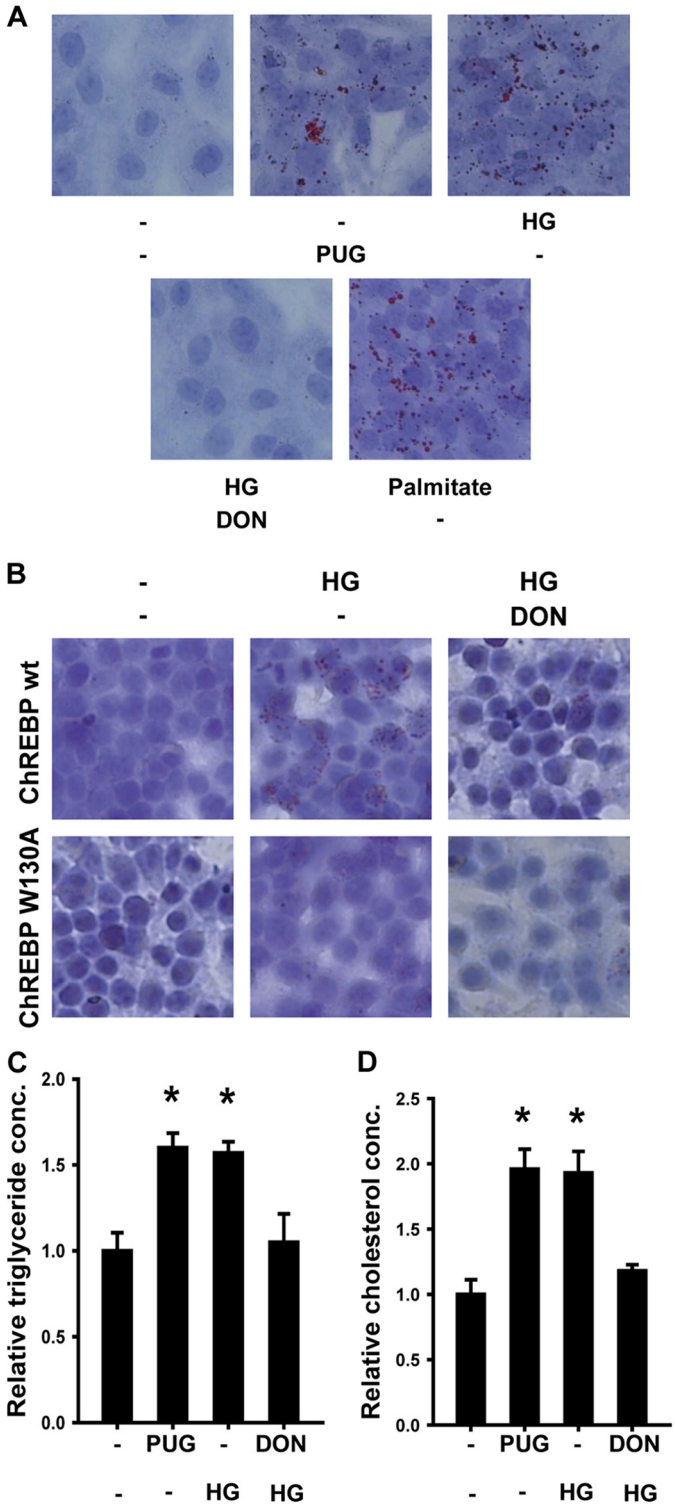

FIGURE 6. ***O*-GlcNAcylation of ChREBP induces lipid accumulation in mesangial cells.** Non-transfected mesangial cells (*A*) and wild type- or mutant ChREBP-transfected HEK293 cells (*B*) were treated with PUGNAc, DON, HG, or 500 μM palmitic acid, as indicated. Oil Red O staining indicated the lipid droplets as a *red color*. Cells were counterstained with hematoxylin (*blue*). Representative images are shown (magnification, ×200). *C* and *D*, extracted triglyceride or cholesterol from mesangial cells, treated with PUGNAc, HG, or HG with DON for 24 h were detected by triglyceride or cholesterol quantification with a colorimetric kit, respectively. The mean ± S.E. (*error bars*) of three experiments denotes relative concentration. *, $p < 0.05$ *versus* control.

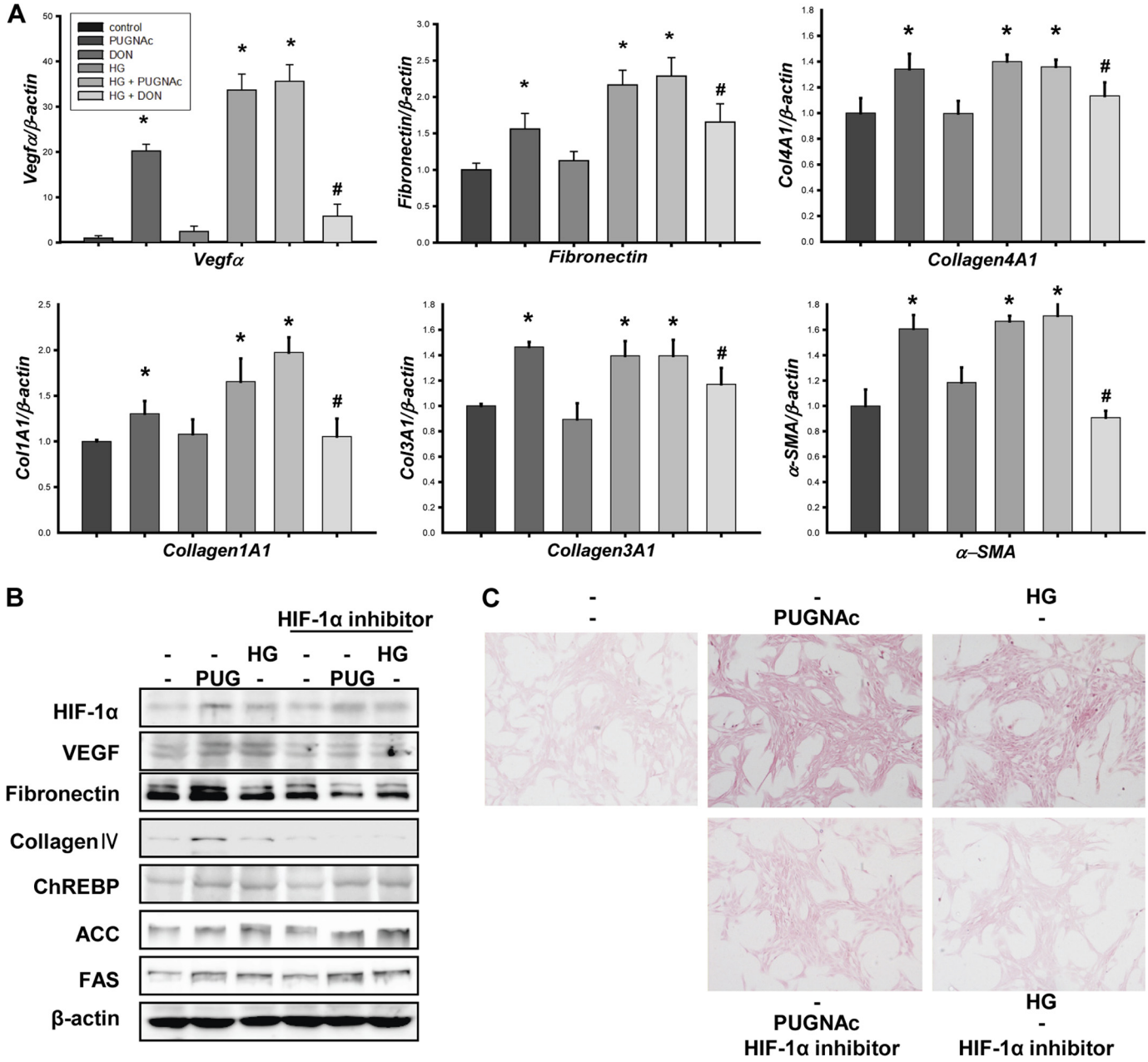

FIGURE 7. **HIF-1α induced by ChREBP regulates fibrosis in mesangial cells under high glucose.** *A*, mesangial cells were treated with 100 μM PUGNAc or 40 μM DON and HG for 16 h. The mRNA levels were determined by real-time PCR. Values are the mean ± S.E. (*error bars*) of three individual experiments. *, $p < 0.05$ *versus* control. #, $p < 0.05$ *versus* HG only. *B* and *C*, mesangial cells were pretreated with 100 nM HIF-1α inhibitor. After 15 min, cells were treated with HG or PUGNAc for an additional 24 h. *B*, protein levels were determined by immunoblotting. *C*, histological visualization of mesangial cell fibrosis was examined by picrosirius red staining. Representative images are shown (magnification, ×400).

(Fig. 8, *B* and *C*). These results confirmed the augmented ChREBP glycosylation *in vivo* diabetic model as well as the *in vitro* model.

DISCUSSION

SREBP has been reported to mediate renal lipotoxicity. Levi's group (37–41) has reported that maladaptive renal cell lipid metabolism is driven by injury-induced type I and II diabetes, caloric overload, and aging. They showed an increase of SREBP-1 and FAS expression, resulting in increased triglyceride accumulation in the glomerular, tubular, and tubulointerstitial cells of streptozotocin-induced rats (37). In addition, along with SREBP-1c, they demonstrated increased ChREBP activity in type 1 diabetic kidney of OVE26 mice (41). However, there is little evidence that elucidates the interaction between ChREBP and lipid metabolism under a hyperglycemic condition in the kidney.

In this study, we investigated the role of ChREBP *O*-GlcNAcylation, a consequence of enhanced HBP flux, in *in vitro* models of diabetic nephropathy using mesangial cells. ChREBP is a major mediator of glucose action in the control of both glycolysis and lipogenesis in the liver (42–44). Thus, we focused on lipogenesis, particularly in mesangial cells, because ChREBP expression was augmented in the kidneys of rats with

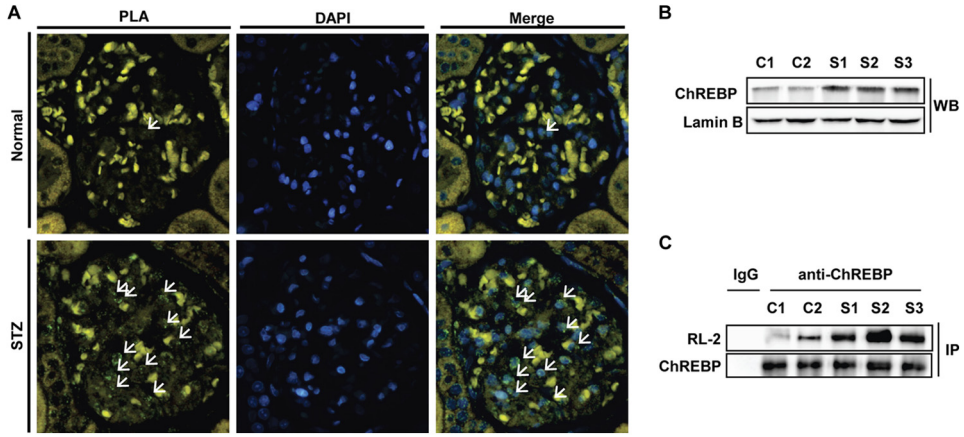

FIGURE 8. ***O*-GlcNAcylated ChREBP was elevated in mesangium of streptozotocin-induced diabetic rats compared with those of control mice.** *A*, an *in situ* proximity ligation assay revealed markedly increased *O*-GlcNAc-modified ChREBP in the mesangium of STZ-induced hyperglycemic rats compared with those of normal rats. Immunofluorescence confocal images show the endogenous ChREBP modified with *O*-GlcNAc as *green dots* (indicated with *white arrows*; magnification, ×400). Nuclei were counterstained with DAPI (*blue*). *B*, nuclear ChREBP protein levels in kidney cortex of STZ rats or normal rats. Lamin B was used to normalize the quantities of nucleic proteins. *C*, nuclear extractions of kidney cortex were immunoprecipitated (*IP*) with ChREBP antibodies and immunoblotted with ChREBP or RL-2 antibodies.

chronic renal failure (26), and renal lipotoxicity has been implicated in kidney abnormalities (2–6). In the present study, HG, but not palmitic acid, increased expression levels of ChREBP and its target genes (*ACC* and *FAS*); this effect of HG was abolished by overexpression of OGA or treatment with DON. Moreover, HG did not increase LXR activation in mesangial cells. These results suggest that ChREBP *O*-GlcNAcylation mediates lipid accumulation in kidney mesangial cells. Our results are partly in agreement with several previous reports. Recently, Goldberg *et al.* (45) reported that *O*-GlcNAcylation in the HG condition is coupled to profibrotic p38 MAPK signaling in mesangial cells. Degrell *et al.* (46) showed that *O*-linked *N*-acetylglucosamine is present in the glomeruli of patients with diabetic nephropathy. However, the authors did not state that specific factors, such as ChREBP and *O*-GlcNAcylation, induced lipid accumulation. Because ChREBP *O*-GlcNAcylation in the liver has been reported previously (17, 24, 25), we focused on ChREBP *O*-GlcNAcylation in mesangial cells. In this study, we demonstrated that under the HG condition, *O*-GlcNAc transactivation of ChREBP mediates lipid accumulation in mesangial cells. Furthermore, we showed significantly elevated ChREBP *O*-GlcNAcylation in the mesangium of the hyperglycemic *in vivo* model.

The N-terminal segment of ChREBP contains five highly conserved domains designated MCRs, and the W130A mutation in the MCR3 domain is important for glucose activation of ChREBP (31). The novel finding of this study is that the Trp-130 residue in the MCR3 domain of ChREBP is responsible for HG-induced lipid accumulation and lipogenesis in mesangial cells because ChREBP W130A blocked the HG-induced increase in Oil Red O staining and levels of lipogenic proteins. Based on the abolition of transcriptional activities by the W130A mutant, the Trp-130 residue and other residues within MCR3 could influence the environment in which ChREBP is *O*-GlcNAcylated by glucose. Characterization of the relationship between Trp-130 and *O*-GlcNAcylation is important; therefore, we attempted to identify the underlying mechanism. Additionally, the interaction between 14-3-3 and ChREBP with the Trp-130 residue is not altered by either *O*-GlcNAcylation of ChREBP or the *O*-GlcNAc status in mesangial cells, as shown in Fig. 5*B*, suggesting that *O*-GlcNAcylation is irrelevant in the interaction between ChREBP and 14-3-3.

Renal fibrosis is a major characteristic of diabetic glomerulosclerosis. Evidence suggests that diabetic renal fibrosis is associated with an increase in SREBP-1c and ChREBP levels (41). Although research on the function of ChREBP in the kidney is limited, we hypothesized that ChREBP could play a prominent role in renal fibrosis because studies suggest that ChREBP expression is augmented in kidneys of rats with chronic renal failure (26), and HIF-1 signaling is activated by HG through ChREBP in mesangial cells (27). Among many HIF-1 target genes, excess VEGF is considered relevant to the pathogenesis of diabetic nephropathy (34) and focal glomerular sclerosis (34, 35, 47, 48). Several studies have suggested a pivotal role for VEGF in glomerular hypertrophy and extracellular matrix production (47, 48). However, to date, no direct evidence that ChREBP mediates renal fibrosis in the kidney has been presented. Our current results show that under the HG condition, ChREBP *O*-GlcNAcylation is also involved in renal fibrosis, in which the Trp-130 residue is important also.

In summary, the present study highlights the role of ChREBP glycosylation in lipogenesis and renal fibrosis in mesangial cells under the HG condition. We presented a model of the signaling mechanism associated with HG-induced lipid accumulation and renal fibrosis in mesangial cells (Fig. 9). HG induced the cellular *O*-GlcNAc pool and ChREBP *O*-GlcNAcylation, which enhanced the ChREBP level, transcriptional activity, stability, and nuclear localization, thus triggering its target protein signaling, especially that of lipogenic proteins and fibrosis-inducing proteins, which may render mesangial cells susceptible to hyperglycemia. The Trp-130 residue of ChREBP within the MCR domain is an important site in inducing lipogenesis and fibrosis of diabetic nephropathy. These findings could help to determine the role of glucose metabolism in renal pathological conditions and suggest potential targets to prevent the development of mesangial lipotoxicity and sclerosis.

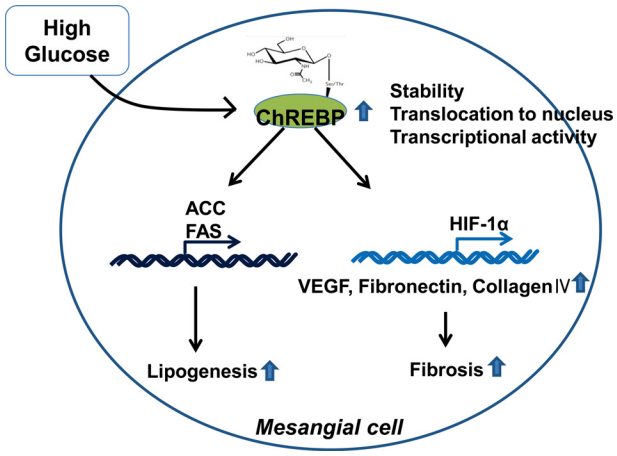

FIGURE 9. **The hypothesized model for the signal pathway involved in the ChREBP-induced lipogenesis and fibrosis in mesangial cells under high glucose.** In mesangial cells, high glucose-induced ChREBP *O*-GlcNAcylation enhanced the ChREBP level, transcriptional activity, stability, and nuclear localization. This, in turn, triggered its target protein signaling, especially that of lipogenic proteins and fibrosis-inducing proteins, which may render mesangial cells susceptible to hyperglycemia.

Acknowledgment—We thank Dr. Howard C. Towle (University of Minnesota) for providing constructs of ChREBP and the luciferase assay.

REFERENCES

1. Sun, Y. M., Su, Y., Li, J., and Wang, L. F. (2013) Recent advances in understanding the biochemical and molecular mechanism of diabetic nephropathy. *Biochem. Biophys. Res. Commun.* **433,** 359–361
2. Oda, H., and Keane, W. F. (1997) Lipids in progression of renal disease. *Kidney Int. Suppl.* **62,** S36–S38
3. Klahr, S., and Harris, K. (1989) Role of dietary lipids and renal eicosanoids on the progression of renal disease. *Kidney Int. Suppl.* **27,** S27–S31
4. Weinberg, J. M. (2006) Lipotoxicity. *Kidney Int.* **70,** 1560–1566
5. Tovar-Palacio, C., Tovar, A. R., Torres, N., Cruz, C., Hernández-Pando, R., Salas-Garrido, G., Pedraza-Chaverri, J., and Correa-Rotter, R. (2011) Proinflammatory gene expression and renal lipogenesis are modulated by dietary protein content in obese Zucker fa/fa rats. *Am. J. Physiol. Renal Physiol.* **300,** F263–F271
6. Kiss, E., Kränzlin, B., Wagenblass, K., Bonrouhi, M., Thiery, J., Gröne, E., Nordström, V., Teupser, D., Gretz, N., Malle, E., and Gröne, H. J. (2013) Lipid droplet accumulation is associated with an increase in hyperglycemia-induced renal damage: prevention by liver X receptors. *Am. J. Pathol.* **182,** 727–741
7. Whelan, S. A., Dias, W. B., Thiruneelakantapillai, L., Lane, M. D., and Hart, G. W. (2010) Regulation of insulin receptor substrate 1 (IRS-1)/AKT kinase-mediated insulin signaling by O-Linked β-*N*-acetylglucosamine in 3T3-L1 adipocytes. *J. Biol. Chem.* **285,** 5204–5211
8. Parker, G. J., Lund, K. C., Taylor, R. P., and McClain, D. A. (2003) Insulin resistance of glycogen synthase mediated by *O*-linked *N*-acetylglucosamine. *J. Biol. Chem.* **278,** 10022–10027
9. Du, X. L., Edelstein, D., Dimmeler, S., Ju, Q., Sui, C., and Brownlee, M. (2001) Hyperglycemia inhibits endothelial nitric oxide synthase activity by posttranslational modification at the Akt site. *J. Clin. Invest.* **108,** 1341–1348
10. Housley, M. P., Rodgers, J. T., Udeshi, N. D., Kelly, T. J., Shabanowitz, J., Hunt, D. F., Puigserver, P., and Hart, G. W. (2008) *O*-GlcNAc regulates FoxO activation in response to glucose. *J. Biol. Chem.* **283,** 16283–16292
11. Anthonisen, E. H., Berven, L., Holm, S., Nygård, M., Nebb, H. I., and Grønning-Wang, L. M. (2010) Nuclear receptor liver X receptor is *O*-GlcNAc-modified in response to glucose. *J. Biol. Chem.* **285,** 1607–1615
12. Hart, G. W., Slawson, C., Ramirez-Correa, G., and Lagerlof, O. (2011) Cross talk between *O*-GlcNAcylation and phosphorylation: roles in signaling, transcription, and chronic disease. *Annu. Rev. Biochem.* **80,** 825–858
13. Slawson, C., Copeland, R. J., and Hart, G. W. (2010) O-GlcNAc signaling: a metabolic link between diabetes and cancer? *Trends Biochem. Sci.* **35,** 547–555
14. Guo, K., Gan, L., Zhang, S., Cui, F. J., Cun, W., Li, Y., Kang, N. X., Gao, M. D., and Liu, K. Y. (2012) Translocation of HSP27 into liver cancer cell nucleus may be associated with phosphorylation and *O*-GlcNAc glycosylation. *Oncol. Rep.* **28,** 494–500
15. Fong, J. J., Nguyen, B. L., Bridger, R., Medrano, E. E., Wells, L., Pan, S., and Sifers, R. N. (2012) β-*N*-Acetylglucosamine (*O*-GlcNAc) is a novel regulator of mitosis-specific phosphorylations on histone H3. *J. Biol. Chem.* **287,** 12195–12203
16. Park, S. Y., Ryu, J., and Lee, W. (2005) *O*-GlcNAc modification on IRS-1 and Akt2 by PUGNAc inhibits their phosphorylation and induces insulin resistance in rat primary adipocytes. *Exp. Mol. Med.* **37,** 220–229
17. Sakiyama, H., Fujiwara, N., Noguchi, T., Eguchi, H., Yoshihara, D., Uyeda, K., and Suzuki, K. (2010) The role of *O*-linked GlcNAc modification on the glucose response of ChREBP. *Biochem. Biophys. Res. Commun.* **402,** 784–789
18. Ferré, P., and Foufelle, F. (2010) Hepatic steatosis: a role for *de novo* lipogenesis and the transcription factor SREBP-1c. *Diabetes Obes. Metab.* **12,** 83–92
19. Dentin, R., Girard, J., and Postic, C. (2005) Carbohydrate responsive element binding protein (ChREBP) and sterol regulatory element binding protein-1c (SREBP-1c): two key regulators of glucose metabolism and lipid synthesis in liver. *Biochimie* **87,** 81–86
20. Stoeckman, A. K., Ma, L., and Towle, H. C. (2004) Mlx is the functional heteromeric partner of the carbohydrate response element-binding protein in glucose regulation of lipogenic enzyme genes. *J. Biol. Chem.* **279,** 15662–15669
21. Decaux, J. F., Antoine, B., and Kahn, A. (1989) Regulation of the expression of the L-type pyruvate kinase gene in adult rat hepatocytes in primary culture. *J. Biol. Chem.* **264,** 11584–11590
22. Towle, H. C., Kaytor, E. N., and Shih, H. M. (1997) Regulation of the expression of lipogenic enzyme genes by carbohydrate. *Annu. Rev. Nutr.* **17,** 405–433
23. Jeong, Y. S., Kim, D., Lee, Y. S., Kim, H. J., Han, J. Y., Im, S. S., Chong, H. K., Kwon, J. K., Cho, Y. H., Kim, W. K., Osborne, T. F., Horton, J. D., Jun, H. S., Ahn, Y. H., Ahn, S. M., and Cha, J. Y. (2011) Integrated expression profiling and genome-wide analysis of ChREBP targets reveals the dual role for ChREBP in glucose-regulated gene expression. *PLoS One* **6,** e22544
24. Guinez, C., Filhoulaud, G., Rayah-Benhamed, F., Marmier, S., Dubuquoy, C., Dentin, R., Moldes, M., Burnol, A. F., Yang, X., Lefebvre, T., Girard, J., and Postic, C. (2011) *O*-GlcNAcylation increases ChREBP protein content and transcriptional activity in the liver. *Diabetes* **60,** 1399–1413
25. Ido-Kitamura, Y., Sasaki, T., Kobayashi, M., Kim, H. J., Lee, Y. S., Kikuchi, O., Yokota-Hashimoto, H., Iizuka, K., Accili, D., and Kitamura, T. (2012) Hepatic FoxO1 integrates glucose utilization and lipid synthesis through regulation of Chrebp *O*-glycosylation. *PLoS One* **7,** e47231
26. Cho, K. H., Kim, H. J., Kamanna, V. S., and Vaziri, N. D. (2010) Niacin improves renal lipid metabolism and slows progression in chronic kidney disease. *Biochim. Biophys. Acta* **1800,** 6–15
27. Isoe, T., Makino, Y., Mizumoto, K., Sakagami, H., Fujita, Y., Honjo, J., Takiyama, Y., Itoh, H., and Haneda, M. (2010) High glucose activates HIF-1-mediated signal transduction in glomerular mesangial cells through a carbohydrate response element binding protein. *Kidney Int.* **78,** 48–59
28. Tsatsos, N. G., and Towle, H. C. (2006) Glucose activation of ChREBP in hepatocytes occurs via a two-step mechanism. *Biochem. Biophys. Res. Commun.* **340,** 449–456
29. Potter, K. A., Simon, J. S., Velagapudi, B., and Capadona, J. R. (2012) Reduction of autofluorescence at the microelectrode-cortical tissue interface improves antibody detection. *J. Neurosci. Methods* **203,** 96–105
30. Slawson, C., Zachara, N. E., Vosseller, K., Cheung, W. D., Lane, M. D., and Hart, G. W. (2005) Perturbations in *O*-linked β-*N*-acetylglucosamine pro-

tein modification cause severe defects in mitotic progression and cytokinesis. *J. Biol. Chem.* **280,** 32944–32956
31. Davies, M. N., O'Callaghan, B. L., and Towle, H. C. (2008) Glucose activates ChREBP by increasing its rate of nuclear entry and relieving repression of its transcriptional activity. *J. Biol. Chem.* **283,** 24029–24038
32. Sakiyama, H., Wynn, R. M., Lee, W. R., Fukasawa, M., Mizuguchi, H., Gardner, K. H., Repa, J. J., and Uyeda, K. (2008) Regulation of nuclear import/export of carbohydrate response element-binding protein (ChREBP): interaction of an α-helix of ChREBP with the 14-3-3 proteins and regulation by phosphorylation. *J. Biol. Chem.* **283,** 24899–24908
33. Amann, K., and Benz, K. (2013) Structural renal changes in obesity and diabetes. *Semin. Nephrol.* **33,** 23–33
34. Ziyadeh, F. N., and Wolf, G. (2008) Pathogenesis of the podocytopathy and proteinuria in diabetic glomerulopathy. *Curr. Diabetes Rev.* **4,** 39–45
35. LeHir, M., and Kriz, W. (2007) New insights into structural patterns encountered in glomerulosclerosis. *Curr. Opin. Nephrol. Hypertens.* **16,** 184–191
36. Wu, T., Zhang, B., Ye, F., and Xiao, Z. (2013) A potential role for caveolin-1 in VEGF-induced fibronectin upregulation in mesangial cells: involvement of VEGFR2 and Src. *Am. J. Physiol. Renal Physiol.* **304,** F820–F830
37. Sun, L., Halaihel, N., Zhang, W., Rogers, T., and Levi, M. (2002) Role of sterol regulatory element-binding protein 1 in regulation of renal lipid metabolism and glomerulosclerosis in diabetes mellitus. *J. Biol. Chem.* **277,** 18919–18927
38. Wang, Z., Jiang, T., Li, J., Proctor, G., McManaman, J. L., Lucia, S., Chua, S., and Levi, M. (2005) Regulation of renal lipid metabolism, lipid accumulation, and glomerulosclerosis in FVBdb/db mice with type 2 diabetes. *Diabetes* **54,** 2328–2335
39. Jiang, T., Wang, Z., Proctor, G., Moskowitz, S., Liebman, S. E., Rogers, T., Lucia, M. S., Li, J., and Levi, M. (2005) Diet-induced obesity in C57BL/6J mice causes increased renal lipid accumulation and glomerulosclerosis via a sterol regulatory element-binding protein-1c-dependent pathway. *J. Biol. Chem.* **280,** 32317–32325
40. Jiang, T., Liebman, S. E., Lucia, M. S., Phillips, C. L., and Levi, M. (2005) Calorie restriction modulates renal expression of sterol regulatory element binding proteins, lipid accumulation, and age-related renal disease. *J. Am. Soc. Nephrol.* **16,** 2385–2394
41. Proctor, G., Jiang, T., Iwahashi, M., Wang, Z., Li, J., and Levi, M. (2006) Regulation of renal fatty acid and cholesterol metabolism, inflammation, and fibrosis in Akita and OVE26 mice with type 1 diabetes. *Diabetes* **55,** 2502–2509
42. Denechaud, P. D., Dentin, R., Girard, J., and Postic, C. (2008) Role of ChREBP in hepatic steatosis and insulin resistance. *FEBS Lett.* **582,** 68–73
43. Iizuka, K., and Horikawa, Y. (2008) ChREBP: a glucose-activated transcription factor involved in the development of metabolic syndrome. *Endocr. J.* **55,** 617–624
44. Denechaud, P. D., Bossard, P., Lobaccaro, J. M., Millatt, L., Staels, B., Girard, J., and Postic, C. (2008) ChREBP, but not LXRs, is required for the induction of glucose-regulated genes in mouse liver. *J. Clin. Invest.* **118,** 956–964
45. Goldberg, H., Whiteside, C., and Fantus, I. G. (2011) *O*-Linked β-*N*-acetylglucosamine supports p38 MAPK activation by high glucose in glomerular mesangial cells. *Am. J. Physiol. Endocrinol. Metab.* **301,** E713–E726
46. Degrell, P., Cseh, J., Mohás, M., Molnár, G. A., Pajor, L., Chatham, J. C., Fülöp, N., and Wittmann, I. (2009) Evidence of *O*-linked *N*-acetylglucosamine in diabetic nephropathy. *Life Sci.* **84,** 389–393
47. Amemiya, T., Sasamura, H., Mifune, M., Kitamura, Y., Hirahashi, J., Hayashi, M., and Saruta, T. (1999) Vascular endothelial growth factor activates MAP kinase and enhances collagen synthesis in human mesangial cells. *Kidney Int.* **56,** 2055–2063
48. Liu, E., Morimoto, M., Kitajima, S., Koike, T., Yu, Y., Shiiki, H., Nagata, M., Watanabe, T., and Fan, J. (2007) Increased expression of vascular endothelial growth factor in kidney leads to progressive impairment of glomerular functions. *J. Am. Soc. Nephrol.* **18,** 2094–2104